Allelic Discrimination for Single Nucleotide Polymorphisms in the Human Scavenger Receptor Class B Type 1 Gene Locus Using Fluorescent Probes, *Doreen Osgood-McWeeney,* Jennifer R. Galluzzi, and Jose M. Ordovas* (JM-USDA Human Nutrition Research Center on Aging at Tufts University, Lipid Metabolism Laboratory, 711 Washington St., Boston, MA 02111; *author for correspondence: fax 617-556-3103, e-mail dosgood@hnrc.tufts.edu)

The scavenger receptor class B type 1 (SR-BI), a multiligand receptor, appears to be a physiologically relevant HDL receptor in rodents *(1, 2)*. To determine its role in humans, the human *SRB1* gene has been characterized *(3, 4)* and its genetic variation investigated in a Caucasian population *(4)*. We have reported three variants, at exons 1 and 8 and intron 5, with allele frequencies >0.1 that have significant associations with lipid and anthropometric variables *(4)*. The exon 1 variant (G→A) was associated with a favorable, antiatherogenic lipid profile in men. Women carriers of the intron 5 variant (C→T) showed a higher body mass index ($P = 0.031$) than those women homozygous for the common (wild-type) allele. The exon 8 variant (C→T) was associated with lower LDL-cholesterol concentrations compared with those homozygous for the common (wild-type) allele. All three variants were single nucleotide polymorphisms (SNPs), and genotyping was carried out by restriction digestion with *Alu*I, *Hae*III, and *Apa*I for exon 1, exon 8, and intron 5, respectively. Because these are the first published associations indicating that SR-BI may play a role in lipid metabolism, these observations need to be examined and confirmed in other populations.

Traditionally, genotyping for genetic mutations has been analyzed by restriction endonuclease digestion and visualized on agarose or polyacrylamide gels. Restriction digestion is an essential procedure in the detection of nucleotide mutations. However, its sensitivity depends on the quality of the amplification of the gene of interest and the staining intensity of the digested products. Furthermore, if no natural restriction site is created or lost, then a cut site must be generated by changing the primer sequence. This can be time-consuming and sometimes difficult to optimize.

Allelic discrimination using the 5′ Nuclease Assay with fluorogenic probes provides a rapid and sensitive method for detecting known mutants or polymorphisms *(5, 6)*. This method combines PCR and mutation detection in a single step. A hybridization probe is cleaved by the 5′ nuclease activity of Taq DNA polymerase only if the specific sequence is successfully amplified. Two TaqMan (PE Applied Biosystems) probes are used, one for each allele. Each probe consists of an oligonucleotide with a 5′ reporter dye and a 3′ quencher dye. The reporter dyes used are 6-carboxy-fluorescein (FAM) and VIC®, and 6-carboxy-tetramethylrhodamine (TAMRA) is used as the quencher dye *(7)*. Initially, the proximity of the quencher suppresses the fluorescent signal given by the reporter through Förster resonance energy transfer *(7)*. The TaqMan probe hybridizes to a smaller 20- to 24mer sequence, which includes the SNP. AmpliTaq Gold (PE Applied Biosystems) enzyme then cleaves the probe with its 5′-3′ nuclease activity. Thus, the reporter dye and quencher dye become separated, causing an increase in the fluorescence intensity of the reporter dye. Our laboratory has reported the implementation of this method using the Perkin-Elmer/Applied Biosystems 7700 Sequence Detection Systems (SDS) and TaqMan reagents with a point mutation in the intestinal fatty acid binding protein *(8)*. We now report the successful implementation of this method in genotyping the SNPs in the human *SRB1* gene locus. The primer and probe sequences used are given in Table 1. PCR was performed in a 10-μL final volume for each individual SNP. The reaction mixture contained 5 μL of TaqMan 2× Universal PCR Master Mix (AmpliTaq Gold polymerase, Amperase uracil-N-glycosylase, dUTP, dGTP, dCTP, dATP, 6-carboxy-x-rhodamine dye, Tris-HCl, KCl, $MgCl_2$), 200 nmol/L FAM-labeled probe, 150 nmol/L VIC-labeled probe, 900 nmol/L reverse primer, 900 nmol/L forward primer, and 2–20 ng of genomic DNA. The thermal cycler program includes one cycle at 50 °C for 2 min to activate uracil-N-gylcosylase, which is added to prevent carryover contamination; one cycle at 95 °C for 10 min to activate the AmpliTaq Gold Polymerase; and then 40 cycles of 95 °C for 15 s for denaturing and 62 °C (for exons 1 and 8) or 69 °C (for intron 5; see Table 1) for 60 s for annealing/extending.

Allelic discrimination was performed on the post-PCR product. The 7700 SDS collects fluorescence data on the samples for ~5 s, and SDS software analyzes the fluorescence, which can be visualized in graph form (Fig. 1 for exon 8). Clusters of points, where each point represents a sample, correspond to a particular genotype or no amplification. For exon 8 genotyping, if there is fluorescence from the reporter (VIC) for the wild-type allele, then the sample is typed as a CC. Fluorescence from only the FAM reporter represents the homozygosity for the mutant allele and is genotyped as TT. Intermediate fluorescence

Table 1. Probe and primer sequences and temperatures for the genotyping of *SRB1* SNPs.

Exon 1 (G→A): anneal temperature, 62 °C
- Forward primer: 5′-GTCCCCGTCTCCTGCCA-3′
- Reverse primer: 5′-CCCAGCACAGCGCACAGTA-3′
- G-Allele probe: 5′-FAM-AGACATG**G**GCTGCTCCGCCA-TAMRA-3′[a]
- A-Allele probe: 5′-VIC-CAGACATG**A**GCTGCTCCGCCA-TAMRA-3′

Intron 5 (C→T) complementary strand G-to-A used: anneal temperature, 69 °C
- Forward primer: 5′-CAAGTGGAACGGGCTGAGCAAGGT-3′
- Reverse primer: 5′-TCTGGTCCCTGCCACTCCCGA-3′
- C-Allele probe: 5′-FAM-AGCCATGGCC**G**GGCCCACC-TAMRA-3′
- T-Allele probe: 5′-VIC-AGCCATGGCC**A**GGCCCACCC-TAMRA-3′

Exon 8 (C→T): anneal temperature, 62 °C
- Forward primer: 5′-CCCCCTTGTTTCTCTCCCAT-3′
- Reverse primer: 5′-AGGCCAGTCACCGCTTCTG-3′
- C-Allele probe: 5′-VIC-CCTCAACGC**C**GACCCGGTT-TAMRA-3′
- T-Allele probe: 5′-FAM-TTCCTCAACGC**T**GACCCGGTTC-TAMRA-3′

[a] Bases in bold represent point mutations.

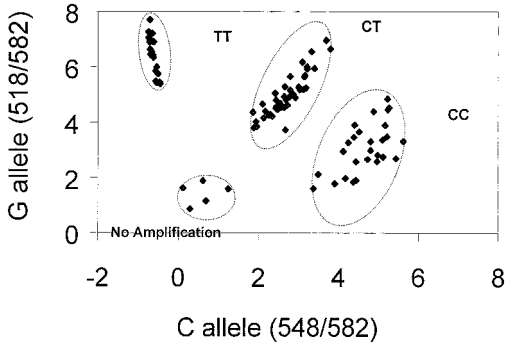

Fig. 1. *SRB1* exon 8 genotyping.

Plot of fluorescence of VIC (C allele, wild-type) and FAM (T allele, mutant). Fluorescence was measured at 518 nm (FAM), 548 nm (VIC), and 582 (TAMRA). To normalize for well-to-well variability in probe concentration, the intensities at 518 and 548 nm were divided by the intensity at 582 nm. *TT*, homozygous mutant; *CT*, heterozygous mutant; *CC*, homozygous wild type; *No Amplification*, no DNA.

from both reporters represents the heterozygous population (CT). Similar genotyping was performed for the exon 1 and intron 5 SNPs (data not shown), with the only difference being the reporters used (see Table 1).

We have genotyped 95 samples, using both fluorescent probes and the traditional enzyme restriction digestion for all three SNPs, and found no disagreement in the genotyping. This method allows for rapid screening for genotyping. Ninety-six samples can be amplified and genotyped in <3 h. Although the system is expensive, long-term savings can be substantial. We have estimated the cost at $1.00 per sample. In addition, there are no hazardous reagents such as ethidium bromide, which is commonly used to visualize restriction digestion products on agarose or acrylamide gels. Moreover, because this method is sensitive and tolerates a broad range of DNA concentrations, there is a high rate for successful genotyping.

This work was supported by Grant HL54776 from the National Heart, Lung, and Blood Institute, and Cooperative Agreement 58-1950-9-001 from the US Department of Agriculture Research Service. We would like to thank Dan Shaffer of Perkin-Elmer for help in designing the primers and probes.

References

1. Krieger, M. The "best" of cholesterols, the "worst" of cholesterols: a tale of two receptors. Proc Natl Acad Sci U S A 1998;95:4077–80.
2. Fidge NH. High density lipoprotein receptors, binding proteins, and ligands. J Lipid Res 1999;40;187–201.
3. Cao G, Garcia CK, Wyne KL, Schultz RA, Parker KL, Hobbs HH. Structure and localization of the human gene encoding SR-BI/CLA-1. Evidence for transcriptional control by steroidogenic factor 1. J Biol Chem 1997;272: 33068–76.
4. Acton S, Osgood D, Donoghue M, Corella D, Pocovi M, Cenarro A, et al. Association of polymorphisms at the SR-BI gene locus with plasma lipid levels and body mass index in a white population. Arterioscler Thromb Vasc Biol 1999;19:1734–43.
5. Livak KJ, Marmaro J, Todd JA. Towards fully automated genome-wide polymorphism screening [Letter]. Nat Genet 1995;9:341–2.
6. Livak KJ. Allelic discrimination using fluorogenic probes and the 5′ nuclease assay. Genet Anal 1999;14:143–9.
7. Perkin-Elmer. TaqMan allelic discrimination protocol, Perkin-Elmer. Foster City, CA: Perkin Elmer, 1998:1–3.
8. Galluzzi JR, Ordovas JM. Genotyping method for point mutation detection in the intestinal fatty acid binding protein, using fluorescent probes. Clin Chem 1999;45:1092–4.

Rapid Detection of Deletion Mutations in Inherited Metabolic Diseases by Melting Curve Analysis with LightCycler, *Tsutomu Aoshima,[1*] Yoshitaka Sekido,[2] Takashi Miyazaki,[2] Mitsuharu Kajita,[1] Shunji Mimura,[1] Kazuyoshi Watanabe,[1] Kaoru Shimokata,[2] and Toshimitsu Niwa[2]* ([1]Department of Pediatrics, Nagoya University School of Medicine, 65 Tsuruma-Cho, Showa-ku, Nagoya 466-8550, Japan; [2] Department of Clinical Preventive Medicine, Nagoya University Daiko Medical Center, 1-1-20 Daikominami, Higashi-ku, Nagoya 461-0047, Japan; * author for correspondence: fax 81-52-719-1132, e-mail taoshima@med.nagoya-u.ac.jp)

Recently, non-gel electrophoresis-requiring, fluorophore probe-based rapid techniques have been introduced to detect known single-point mutations using the LightCycler™ (Roche Molecular Biochemicals) *(1–4)*. This technique provides very rapid analytical time, real-time detection, and visualized images. Many inherited metabolic diseases are caused not only by single-point mutations but also by small deletion mutations. However, no studies have been reported on the detection of such deletion mutations using the LightCycler. Using melting curve analysis with the LightCycler, we have succeeded in rapidly detecting a 2-bp deletion mutation in genomic DNA of a patient with Fabry disease and a 9-bp deletion mutation in cDNA of a patient with carbamoyl-phosphate synthase I (CPS1; EC 6.3.4.16) deficiency.

Fabry disease is an X-linked recessive disorder caused by the deficient activity of α-galactosidase (α-Gal; EC 3.2.1.22). A 15-year-old boy with classical Fabry disease who had suffered from angiokeratoma, acroparesthesias, and attacks of pain in his legs was referred to us. We extracted total RNA from his peripheral blood lymphocytes and analyzed the *α-GAL* gene (*GLA*; GenBank accession no. X14448) by reverse transcription-PCR *(5)*. We sequenced a 1.3-kb PCR product covering the entire coding region and found a 2-bp deletion mutation at nucleotides 11 008–11 009. This change caused a frameshift mutation that had been described previously in another case of the disease *(6)*.

With written informed consent, we examined the patient's relatives, including his mother, his unaffected brother, and his maternal grandmother, to determine whether they carry this mutation. Genomic DNAs were obtained from their peripheral blood lymphocytes, using QIAamp Blood Kit® (Qiagen) according to the manufacturer's instructions.

For fluorescence PCR analysis, we prepared two PCR primers (2Del-S and 2Del-AS) and two fluorescence probes (2Del-F and 2Del-LC; Table 1). A 25mer oligonu-

cleotide probe, 2Del-LC, synthesized by standard phosphoramidite chemistry, was labeled at the 5′ end with LC Red 640 (Roche Molecular Biochemicals) fluorophore and modified at the 3′ end by phosphorylation to avoid extension. Another 20mer oligonucleotide probe, 2Del-F, was synthesized to anneal the region that contained the 2-bp deletion mutation inside, and was labeled at the 3′ end with fluorescein. The distance between the two probes was 1 oligonucleotide. When both the probes hybridize in close proximity, fluorescence resonance energy transfer occurs, producing a specific fluorescence emission of LC-Red at 640 nm (Fig. 1A).

The PCR reaction was performed in a 20-μL mixture containing 2 μL of LightCycler DNA Master Hybridization Probes (Taq DNA polymerase, reaction buffer, dNTP mixture, and 10 mmol/L $MgCl_2$; Roche Molecular Biochemicals), 2.4 μL of 25 mmol/L $MgCl_2$, 0.2 μmol/L each of the probes (2Del-F and 2Del-LC), 0.5 μmol/L each of the primers (2Del-S and 2Del-AS), and 50 ng of DNA. The amplified products were 186 bp in the wild type and 184 bp in the mutated type.

The thermal cycling was carried out as follows: initial denaturation at 95 °C for 30 s, followed by 50 cycles of denaturation at 95 °C for 0 s, annealing at 56 °C for 0 s, and extension at 72 °C for 4 s. The ramp rate was set at 20 °C/s. After amplification was complete, a melting curve in which fluorescence (F) was plotted against temperature (T), was obtained by holding at 95 °C for 30 s and then at 45 °C for 20 s, followed by heating slowly at 0.2 °C/s to 85 °C with continuous collection of fluorescence at 640 nm. It took ~30 min for this thermal cycling. The negative derivative of the fluorescence with respect to temperature ($-dF/dT$) was plotted against temperature.

Derivative melting curves demonstrated a clear difference between their genotypes (Fig. 1B). The curves of the unaffected brother and maternal grandmother showed a wild-type pattern with peaks at 65.5 and 64.7 °C, respectively. On the other hand, because the 2-bp internal deletion decreased the melting temperature (T_m), the patient with Fabry disease showed a single peak at 60.3 °C, which is ~5 °C lower than the peaks in the wild type, demonstrating that he had the hemizygous mutation of the *α-GAL* gene. His mother showed a heterozygous pattern with two peaks at 59.9 and 65.7 °C, demonstrating that she was a carrier of the disease.

CPS1 deficiency is an autosomal recessive disorder caused by the deficient activity of CPS1, affecting the first enzyme step in the urea cycle. We investigated a boy with the neonatal type of the disease, who showed a low activity of CPS1 in the liver and died at age 28 because of severe hyperammonemia. After extracting total RNA from the liver at autopsy, we analyzed the *CPS1* gene (GenBank accession no. Y15793) by reverse transcription-PCR. We synthesized 10 pairs of primer sets to cover the entire coding region (4.5 kb) and performed heteroduplex analysis with MDE™ gel (FMC). The aberrant bands were subcloned into pGEM-T easy plasmid (Promega) and sequenced. Because a 9-bp in-frame deletion from nucleotide 832 to nucleotide 840 was identified in the cDNA, we amplified a genomic DNA fragment and found a G-to-C transition at nucleotide 840. Thus, we showed that this splicing abnormality was attributable to a point mutation located at the end of an exon-intron boundary at the donor site; the same mutation had been reported previously *(7)*. Because we also detected a novel nucleotide substitution on the other allele (Aoshima et al., in preparation), he was shown to be a compound heterozygote with two point mutations.

SYBR™ Green I dye is a DNA double-strand-specific dye, and its fluorescence emission at 530 nm is greatly enhanced by its binding to double-stranded DNA (Fig. 1C). Using this dye, we tested whether products that differ in T_m caused by a deletion can be identified. For fluorescence PCR analysis of the 9-bp deletion, we prepared two PCR primers (9Del-AS and 9Del-AS; Table 1), and three templates; two were the reverse transcription products of the total RNA isolated from the liver of a patient with CPS1 deficiency and a patient with ornithine transcarbamoylase deficiency (as a control); a plasmid containing the homozygous 9-bp deletion mutation was used. The PCR was performed in a 20-μL mixture containing 2 μL of LightCycler DNA Master SYBR Green (Taq DNA polymerase, reaction buffer, dNTP mixture, SYBR Green I dye, and 10 mmol/L $MgCl_2$; Roche Molecular Biochemicals), 2.4 μL of 25 mmol/L $MgCl_2$, 0.5 μmol/L each of the primers (9Del-AS and 9Del-AS), and

Table 1. Oligonucleotides as PCR primers and hybridization probes.

Name	Role	Position	Sequence (5′ → 3′)	Modification
α-GAL				
2Del-S	PCR primer	10 928[a]	GGGCCACTTATCACTAGTTGC	None
2Del-AS	PCR primer	11 114	TGATGAAGCAGGCAGGAT	None
2Del-F	Probe	10 995	GTGGGAACGACCTCTCTCAG	3′-Fluorescein
2Del-LC	Probe	11 016	CTTAGCCTGGGCTGTAGCTATGATA	5′-LC Red 640 3′-Phosphorylation
CPS1				
9Del-S	PCR primer	811[b]	GCAGAACCACTAATTCAG	None
9Del-AS	PCR primer	865	GCTCCTTGCGATCACTCT	None

[a,b] Positions of primers and probes at the 5′ termini, according to GenBank accession number: [a] X14448 for *α-GAL* and [b] Y15793 for *CPS1*.

50 ng of the templates. The amplified products were 55 bp in the wild type and 46 bp in the mutated type. The thermal cycling was carried out under the above conditions except that the extension was at 72 °C for 1 s and the fluorescence was monitored at 530 nm.

Derivative melting curves demonstrated a clear difference between the genotypes (Fig. 1D). The curve of the control showed a wild-type pattern with a single peak at 76.6 °C. On the other hand, because the 9-bp internal deletion decreased its T_m, the plasmid containing the homozygous mutation showed a single peak at 74.9 °C, 1.8 °C lower than the wild type. The patient with CPS1 deficiency showed a heterozygous pattern with two peaks at 74.9 and 76.6 °C.

In this study, we first demonstrated that deletions of small nucleotides can be detected rapidly and easily by fluorophore techniques. We could distinguish the genotypes in a family of Fabry disease. The probe, 2Del-F, which contains the deletion site, hybridized to the mutation template, probably forming a loop with the surplus nucleotides. Therefore, it melted off from the mutation template at a lower temperature than from the wild-type template. This technique can be applied to cases with deletion mutations of larger numbers of nucleotides. The T_m of a PCR product depends on the length itself and GC content. If the difference between the T_ms of the PCR products are large, they can be distinguished from each other using only SYBR Green I dye, as shown in the detection of the 9-bp deletion in CPS1 deficiency. This is a very simple procedure that does not require the designing of specific hybridization probes. However, the deletion must be enough large compared with the whole fragment or contain a high GC content to influence the T_m. For example, in the case of this 9-bp deletion, if the PCR products are 100 bp, the difference of T_m between the mutation and the wild type will be 0.6 °C, which is not detectable. Although the two mutations in this study are not common, we believe that this technique can be widely utilized for rapid and facile screening of the other diseases that have common deletion mutations.

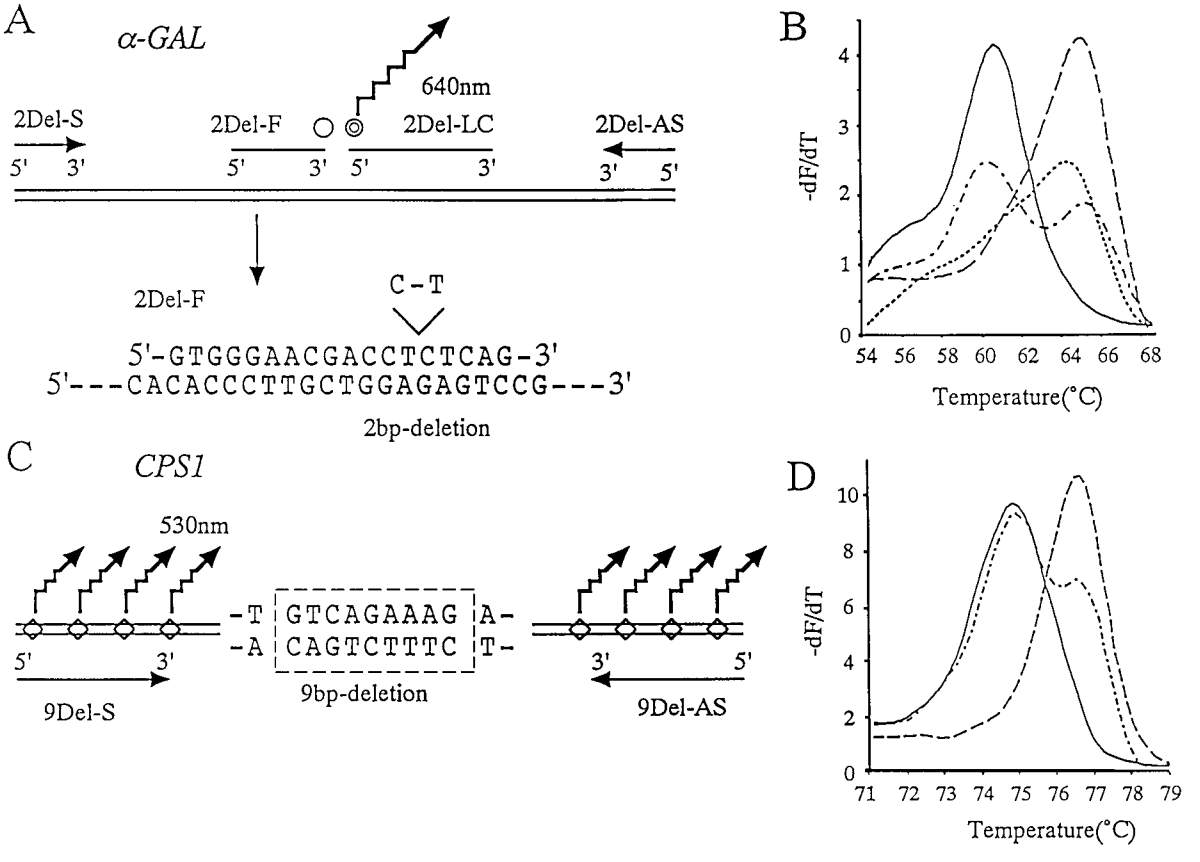

Fig. 1. Schematic illustration of PCR primers and fluorescence probes for α-*GAL* (*A*) and *CPS1* (*C*) and derivative melting curves for genotyping of α-*GAL* (*B*) and *CPS1* (*D*).

(*A*), fragment of α-*GAL* amplified by the two primers (2Del-S and 2Del-AS) is 186 bp in the wild type. When the fluorescence probes (2Del-F and 2Del-LC) hybridize in close proximity, fluorescence resonance energy transfer occurs, producing a specific fluorescence emission at 640 nm. In the mutated type, the two nucleotides of 2Del-F are surplus, forming a loop. ◎, LC-Red; ○, fluorescein. (*B*), derivative melting curves for genotyping of α-*GAL* showed a single peak at high T_m in the wild type and a peak at low T_m in the mutated type. Whereas the curves of the unaffected brother (— — —) and maternal grandmother (- - - - - -) showed a wild-type pattern, the patient (————) showed a hemizygous mutation pattern. The patient's mother (— - — - —) showed a heterozygous pattern with two peaks. (*C*), fragment of *CPS1* amplified by the two primers (9Del-S and 9Del-AS) is 55 bp in the wild type. When SYBR Green I dye binds to double-stranded DNA, it produces the specific fluorescence emission at 530 nm. ◇, SYBR Green I dye. (*D*), derivative melting curves for genotyping of *CPS1* showed a single peak at high T_m in the wild type and a peak at low T_m in the mutated type. The patient with ornithine transcarbamoylase deficiency (— — —) showed a wild-type pattern, the plasmid (————) showed a homozygous mutation pattern, and the patient with CPS1 deficiency (— - — - —) showed a heterozygous mutation pattern with two peaks.

References

1. Lay MJ, Wittwer CT. Real-time fluorescence genotyping of factor V Leiden during rapid-cycle PCR. Clin Chem 1997;43:2262–7.
2. Bernard PS, Lay MJ, Wittwer CT. Integrated amplification and detection of the C677T point mutation in the methylenetetrahydrofolate reductase gene by fluorescence resonance energy transfer and probe melting curves. Anal Biochem 1998;255:101–7.
3. Kyger EM, Krevolin MD, Powell MJ. Detection of the hereditary hemochromatosis gene mutation by real-time fluorescence polymerase chain reaction and peptide nucleic acid clamping. Anal Biochem 1988;260:142–8.
4. von Ahsen N, Schutz E, Armstrong VW, Oellerich M. Rapid detection of prothrombotic mutations of prothrombin (G20210A), factor V (G1691A), and methylenetetrahydrofolate reductase (C677T) by real-time fluorescence PCR with the LightCycler. Clin Chem 1999;45:694–6.
5. Miyazaki T, Kajita M, Ohmori S, Mizutani N, Niwa T, Murata Y, et al. A novel mutation (E358K) in the α-galactosidase A gene detected in a Japanese family with Fabry disease. Hum Mutat 1998;Suppl 1:S139–40.
6. Germain D, Biasotto M, Tosi M, Meo T, Kahn A, Poenaru L. Fluorescence-assisted mismatch analysis (FAMA) for exhaustive screening of the α-galactosidase A gene and detection of carriers in Fabry disease. Hum Genet 1996;98:719–26.
7. Hoshide R, Matsuura T, Haraguchi Y, Endo F, Yoshinaga M, Matsuda I. Carbamyl phosphate synthase I deficiency. One base substitution in an exon of the *CPSI* gene causes a 9-basepair deletion due to aberrant splicing. J Clin Investig 1993;91:1884–7.

Rapid Determination of Total Homocysteine in Blood Spots by Liquid Chromatography-Electrospray Ionization-Tandem Mass Spectrometry, *Klaus Gempel,[1*] Klaus-Dieter Gerbitz,[1] Bruno Casetta,[2] and Matthias F. Bauer[1]* ([1] Institut für Klinische Chemie, Molekulare Diagnostik und Mitochondriale Genetik, Academic Hospital München-Schwabing, Kölner Platz 1, 80804 Munich, Germany; [2] P.E. Biosystems, Via Tiepolo, 24, 20052 Monza, Italy; * author for correspondence: fax 49-(0)89-3068-3911, e-mail Klaus.Gempel@lrz.uni-muenchen.de)

The determination of total homocysteine (tHcy) plays an important role in diagnosis and therapy of folate and cobalamin (vitamin B_{12}) deficiencies. In addition, it is now widely accepted that increased tHcy is an independent risk factor for thromboembolism and cardiovascular disease, including coronary occlusive disease *(1–3)*.

Although the causal role of Hcy in the development of vascular occlusive disease has yet to be determined, prospective intervention trials that will effectively lower total plasma Hcy currently are in progress *(4)*. As a result, various analytical methods have been established to measure tHcy in serum or plasma *(5–10)*. We have established a more rapid protocol suitable for accurately measuring tHcy in hemolysates by use of liquid chromatography-electrospray ionization-tandem mass spectrometry (LC/MS/MS). The LC/MS/MS method circumvents the disadvantages of time-consuming derivatization and allows the processing of >400 samples per day.

Blood was collected in hemolysate tubes that keep the tHcy concentration constant for at least 48 h at room temperature *(11)*. For longer time periods, the hemolysate was stored at −20 °C. Hemolysate (20 μL) was pipetted onto filter paper (Neonatal Screening Card; Schleicher & Schuell). For each sample, two spots (equivalent to 4.7 μL) were punched out and incubated for 15 min at room temperature with a mixture of 20 μL of reducing agent (500 mmol/L dithiothreitol in doubly distilled water) and of 20 μL of internal standard {0.0025 mmol/L D,L-[3,3,3′,3′,4,4,4′,4′-$^2H_8$]-homocystine in HCl-acidified water (M_r 276.33, isotopic purity >98%; Cambridge Isotopes Laboratories)}. tHcy was extracted by the addition of 200 μL of acetonitrile containing 1 mL/L formic acid and 0.5 mL/L trifluoroacetic acid and vortex-mixing for 1 min. Supernatant (4 μL) was loaded onto a Supelcosil™ Cyano column (30 × 3 mm, 3 μm bead size) and eluted with a mixture of 700 mL/L acetonitrile-300 mL/L water containing 0.15 mL/L formic acid at a flow rate of 0.4 mL/min. Unattended sample loading was accomplished using a Perkin-Elmer Series 200 autosampler in combination with a Perkin-Elmer LC pump.

A Perkin-Elmer Sciex API 365 LC/MS/MS benchtop triple quadrupole mass spectrometer operating in positive ion mode was used to analyze the eluate. Ionization was achieved with a turbo ion spray device with pneumatically assisted evaporation operating at an ion spray voltage of +5000 V. The TurboIon gas temperature was set to 350 °C at a flow rate of 8 L/min. The operating conditions yielded a protonated molecular ion of Hcy (*m/z* 136.1) in single MS mode (Fig. 1). In MS/MS mode, Hcy yielded a prominent fragment at *m/z* 90 when a collision gas pressure of 1.067 Pa and a collision energy of 15 eV were applied. Ion transitions monitored in the selected reaction monitoring mode were as follows: 136→90 for Hcy and 140→94 for the internal standard.

Mass spectral analysis of Hcy-containing serum pretreated with dithiothreitol was performed in the product ion mode of the LC/MS/MS (Fig. 1A). The most prominent fragment was produced by a neutral loss of formic acid (loss of 46), giving rise to a product ion of *m/z* 90. This *m/z* 90 ion was further fragmented, with fragmentation products visible at *m/z* 73 and *m/z* 56, which correspond to a neutral loss of ammonia (NH_3, loss of 17) and hydrogen sulfide (H_2S, loss of 34), respectively. This fragmentation pattern was confirmed by the product ion spectrum of D,L-[3,3,3′,3′,4,4,4′,4′-$^2H_8$]-homocystine, which showed essentially the same fragments with a mass shift of +4 attributable to deuterization of the backbone carbon atoms (data not shown).

Potentially interfering substances were removed by chromatography on a short cyano column before the electrospray, which produced symmetrical peaks for Hcy and its internal standard at virtually identical retention times (Fig. 1B). The signal-to-noise ratio of a serum containing 5.5 μmol/L tHcy measured by HPLC with fluorescence detection was calculated as 60. Thus, the detection limit at a signal-to-noise ratio of 5 was calculated to be 0.5 μmol/L. Chromatography and mass spectrometric detection was performed within 3 min, allowing the processing of 20 samples per hour.

For calibration, stabilized hemolysates with low endogenous tHcy were supplemented with D,L-Hcy (M_r 135.18; Sigma-Aldrich). The calibration curves for Hcy quantification were obtained by plotting the peak area ratio for the *m/z* 136→90:140→94 ion pairs vs the concentration of

tHcy (in the range 3.5–60 μmol/L). Calibration curves were analyzed by unweighted least-squares linear regression analysis and were linear over the range studied ($y = 0.024x + 0.033$; $S_{y|x} = 0.039$; $r = 0.998$; n = 6). Within-run precision was determined for a series of 10 spots on paper prepared from samples with low, intermediate, and high concentrations of tHcy; the means ± SD (CV) were 3.5 ± 0.37 μmol/L (11%), 8.6 ± 0.85 μmol/L (9.9%), and 24.9 ± 2.08 μmol/L (8.4%), respectively. Between-run precision was 10.7 ± 1.11 μmol/L (10%). Calibrators, quality-control samples, and patient samples were all spotted, eluted, and determined in exactly the same manner.

To determine the accuracy of this method, we analyzed different hemolysates with endogenous tHcy in the low, medium, and upper reference range that were supplemented with different concentrations of D,L-Hcy. The recoveries of added D,L-Hcy were 72–129%, with a total mean ± SD of 105.5% ± 18.3%.

Further validation of the method was done by comparing the tHcy values of unselected patients determined by reversed-phase HPLC with fluorometric detection to the LC/MS/MS method. The reference range of tHcy in hemolysates determined by HPLC was <9 μmol/L, well in accordance with previously published results *(11)*. Comparison of HPLC (x) and LC/MS/MS (y) revealed a correlation coefficient $r = 0.9296$ with a slope of 1.17. The y-axis intercept was −1.62, and the standard deviation of residuals ($S_{y|x}$) was 1.67. The mean ± SD of the HPLC and LC/MS/MS determinations were 7.01 ± 3.58 and 6.60 ± 4.51 μmol/L, respectively (n = 79 samples).

In conclusion, we have developed and validated a fast, easy, and reliable method to determine tHcy from small amounts of hemolysate or plasma by stable isotope dilution-tandem mass spectrometry. The method avoids derivatization of the Hcy; instead, a simple solid-phase extraction is performed within minutes from filter cards used for neonatal screening. Except for the deuterated internal standard, no expensive reagents are necessary. Cleaning of the sample is achieved by a short in-line preanalytical chromatography column. The method is suitable for determination in stabilized hemolysates, thereby offering the advantage of sample stability for 48 h at room temperature and preventing the significant increase of tHcy in EDTA plasma if it is not immediately separated from the erythrocytes. Finally, because the turnaround time of the method is <3 min per sample, it is well suited for clinical trials in which large numbers of samples must be handled daily.

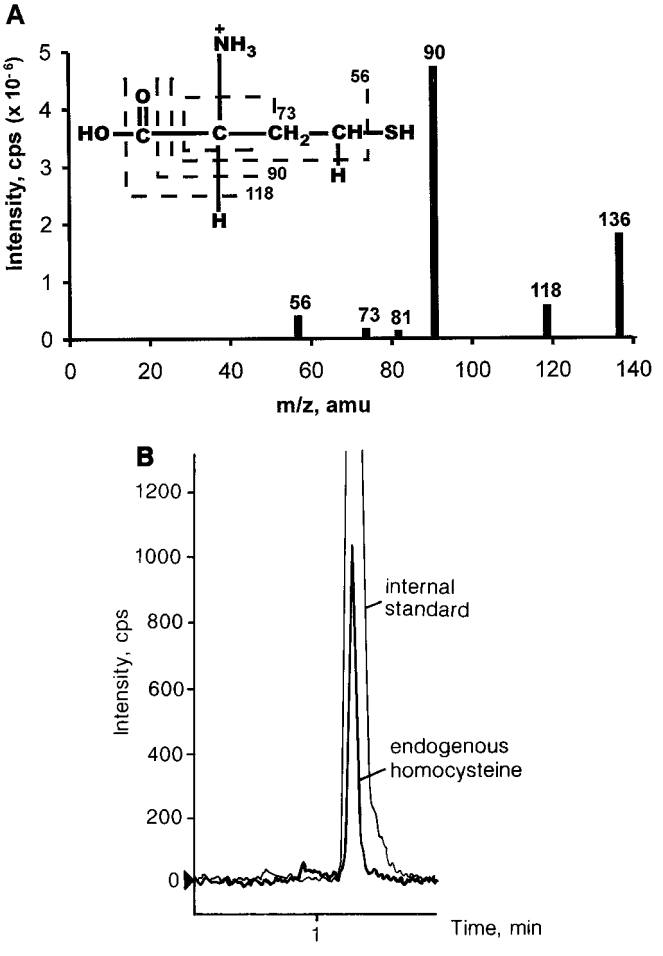

Fig. 1. Product ion spectrum of tHcy ($[M+H]^+$ 136) in serum at a collision energy of 15 eV (*A*) and chromatogram of endogenous tHcy and its corresponding deuterated internal standard detected in the selected reaction monitoring mode (*B*).

The precursor/product ion pairs for unlabeled tHcy and the labeled internal standard were 136→90 and 140→94, respectively. *cps*, counts per second; *amu*, atomic mass units.

We gratefully acknowledge Iris Bieger and Elisabeth Jost for excellent technical assistance.

References

1. Stampfer MJ, Malinow MR, Willett WC, Newcomer LM, Upson B, Ullmann D, et al. A prospective study of plasma homocyst(e)ine and risk of myocardial infarction in US physicians. JAMA 1992;268:877–81.
2. Wu LL, Wu J, Hunt SC, James BC, Vincent GM, Williams RR, et al. Plasma homocyst(e)ine as a risk factor for early familial coronary artery disease. Clin Chem 1994;40:552–61.
3. Nygard O, Vollset SE, Refsum H, Stensvold I, Tverdal A, Nordrehaug JE, et al. Total plasma homocysteine and cardiovascular risk profile. The Hordaland Homocysteine Study. JAMA 1995;274:1526–33.
4. Clarke R, Collins R. Can dietary supplements with folic acid or vitamin B_6 reduce cardiovascular risk? Design of clinical trials to test the homocysteine hypothesis of vascular disease. J Cardiovasc Risk 1998;5:249–55.
5. Araki A, Sako Y. Determination of free and total homocysteine in human plasma by high-performance liquid chromatography with fluorescence detection. J Chromatogr 1987;422:43–52.
6. Refsum H, Ueland PM, Svardal AM. Fully automated fluorescence assay for determining total homocysteine in plasma. Clin Chem 1989;35:1921–7.
7. Ueland PM, Refsum H, Stabler SP, Malinow MR, Andersson A, Allen RH. Total homocysteine in plasma or serum: methods and clinical applications. Clin Chem 1993;39:1764–79.
8. Pietzsch J, Julius U, Hanefeld M. Rapid determination of total homocysteine in human plasma by using N-(O,S)-ethoxycarbonyl ethyl ester derivatives and gas chromatography-mass spectrometry. Clin Chem 1997;43:2001–4.
9. Causse E, Siri N, Bellet H, Champagne S, Bayle C, Valdiguie P, et al. Plasma homocysteine determined by capillary electrophoresis with laser-induced fluorescence detection. Clin Chem 1999;45:412–4.
10. Magera MJ, Lacey JM, Casetta B, Rinaldo P. Method for the determination of total homocysteine in plasma and urine by stable isotope dilution and electrospray tandem mass spectrometry. Clin Chem 1999;45:1517–22.
11. Probst R, Brandl R, Blumke M, Neumeier D. Stabilization of homocysteine concentration in whole blood. Clin Chem 1998;44:1567–9.

Detection of *p53* Polymorphism at Codon 72 by PCR and Allele-specific Oligonucleotide Hybridization on Microtiter Plates, *Dan Tong,[1] Elisabeth Kucera,[1] Margit Stimpfl,[1] Heinz Kölbl,[1] Sepp Leodolter,[1,2] and Robert Zeillinger[1*]* ([1] University of Vienna, Department of Obstetrics and Gynecology, Division of Gynecology, at the General Hospital of Vienna, A-1090 Vienna, Austria; [2] Ludwig-Boltzmann Institute for Gynecological Oncology and Reproductive Medicine, A-1090 Vienna, Austria; * address correspondence to this author at: University of Vienna, Department of Obstetrics and Gynecology, Molecular Oncology Group, Waehringer Guertel 18-20, EBO 05, A-1090 Vienna, Austria; fax 43-1-40400-7832, e-mail robert.zeillinger@akh-wien.ac.at)

The *p53* tumor suppressor gene lies on chromosome 17p and encodes a nuclear phosphoprotein. Wild-type p53 protein can suppress cellular transformation and proliferation *(1, 2)*. Mutations in the *p53* gene are the most common genetic alteration in human cancers *(3)*. More than one-half of all human cancers show either absence of the p53 protein function or mutations in the gene. Mutant and wild-type p53 may oligomerize, thereby disrupting the function of the tetrameric complex *(4)*. Codon 72 of the *p53* gene was found to be a site of frequent polymorphism *(5)*. The frequencies of allelic variants at this codon not only differ among different ethnic groups *(6, 7)*, they are also associated with cancer susceptibility *(8–10)*.

A relationship between viral infection and cancer has been found. It has been reported that adenovirus E1b 55-kDa protein and human papillomavirus E6 protein can bind to and inactivate p53 protein *(11, 12)*. Targeting of p53 by these viruses prevents cell death and induces the cellular proliferation that is necessary for viral replication. The development of most cervical carcinomas has been shown to be associated with human papillomavirus (HPV) types 16 and 18. The E6 oncoprotein encoded by HPV types 16 and 18 has been found to promote the degradation of p53 *(13)*. Recently, it was suggested that the arginine form at codon 72 of *p53* was more susceptible to E6-mediated degradation than the proline form. Individuals homozygous for the arginine form at codon 72 were approximately sevenfold more susceptible to HPV-associated tumorigenesis than heterozygotes *(14)*.

We established a PCR and microtiter plate-based hybridization assay for the detection of the codon 72 polymorphism in *p53*. The system was evaluated with DNA from cell lines with known allelic information. We examined DNA from 105 cervical carcinoma patients and 133 healthy female volunteers, who were representative for the Austrian population.

EDTA-blood samples from 105 cervical carcinoma patients and 133 healthy volunteers were collected at the Department of Obstetrics and Gynecology, University of Vienna, from 1984 to 1998. The median age of the cervical carcinoma patients was 49 years (range, 25–92 years), whereas the median age of the control group was 54 years (range, 21–77 years). In addition, all patients were matched for ethnic background and represented the typical Austrian population. Informed consent was obtained from all patients, and all procedures were approved by the institute's responsible committee.

Breast cancer cell lines T-47D, BT-549, BT-483, CAMA-1, DU4475, Hs 578.T, SK-BR-3, and MCF-7, and ovarian cancer cell lines OVCAR-3 and ES-2 were purchased from American Type Culture Collection. All cell lines were cultured according to the instructions from American Type Culture Collection.

DNA was isolated from blood and cell lines by commercially available kits (DNA Extraction Systems I and II; ViennaLab).

Sense primer 5′-ATGGATGATTTGATGCTGTC-3′ and antisense primer 5′-AGAAGCCCAGACGGAAAC-3′ were used for the amplification of a DNA fragment containing the polymorphic site at codon 72. The antisense primer was labeled with fluorescein. For PCR, 30 ng of DNA was used as template in a total volume of 30 μL. The reaction mixture included 15 pmol of both sense and antisense primers, 250 μmol/L dNTPs (ViennaLab), 3.0 μL of 10× amplification buffer (10 mmol/L Tris-HCl, pH 9.0, 50 mmol/L KCl, 0.1 g/L gelatin, 1.5 mmol/L $MgCl_2$, 1.0 mL/L Triton X-100; ViennaLab) and 1.0 U of Super Taq Polymerase (HT Biotechnology). PCR was performed on a Perkin-Elmer GeneAmp PCR system 9600 with 40 cycles at 94 °C for 30 s, 52 °C for 30 s, and 72 °C for 30 s. All reactions were preceded by a primary denaturation step at 94 °C for 1 min. PCR product (5 μL) was then resolved on 3% agarose gels containing 0.1 mL/L SYBR Green I (Molecular Probes). Gels were excited with 254 nm transilumination.

Oligonucleotides were designed to specifically hybridize either with PCR products from the *p53* Pro^{72} isoform (5′-GCTCCCCCCGTGGC-3′) or the Arg^{72} isoform (5′-CTGCTCCCCGCGTG-3′). The probes were 5′ labeled with biotin. The detection of the *p53* polymorphism was carried out using the Universal Gene Mutation Detection Kit (ViennaLab). Briefly, 10 μL of PCR product was denatured in an alkaline buffer and added to 100 μL of Tris-based hybridization buffer containing 5 pmol of specific oligonucleotide in a streptavidin-coated well. Hybridization was carried out at 37 °C for 30 min. After two stringent washes in a buffer containing 0.4× standard saline citrate at 37 °C, an anti-fluorescein horseradish peroxidase complex was added to the well. Then it was incubated at room temperature for 15 min. The well was washed twice with phosphate-buffered saline, and a color developer containing 3,3′,5,5′-tetramethylbenzidine was added to the well. After 15 min of color development, an acidic buffer was added to stop the reaction, and the color intensity was measured at 450 nm with 630 nm as reference.

For system evaluation and to verify the results from microtiter well-based hybridization, PCR products from cell lines and from 20 randomly selected samples were sequenced directly using an ALFexpress DNA sequencer and the Thermo Sequenase fluorescently labeled primer cycle sequencing kit (Amersham Pharmacia Biotech).

Differences in the allelic frequencies of *p53* at codon 72

between the cervical carcinomas and the control group as well as between the Austrian population and other Caucasian populations were examined by the χ^2 test.

DNAs from several breast and ovarian cancer cell lines were used to evaluate our detection system. Allelic information of *p53* at codon 72 in these cell lines was obtained from sequencing. As shown in Fig. 1A, after amplification of template DNAs by PCR, a 223-bp PCR product was generated. Hybridization of these PCR products to the oligonucleotides specific for the *p53* Pro^{72} isoform and the Arg^{72} isoform on microtiter plates generated either a blue-colored positive signal or a colorless negative signal in the wells. Fig. 1A shows that the cell lines T-47D, BT-549, and ES-2 are homozygous for *p53* Pro^{72}, cell lines BT-483, CAMA-1, Hs 578.T, SK-BR-3, and OVCAR-3 are homozygous for Arg^{72}, and the cell line MCF-7 is heterozygous for Pro^{72} and Arg^{72}. This result was in accordance with the results from direct sequencing, confirming that the detection of *p53* polymorphism at codon 72 by PCR and allele-specific hybridization on microtiter plates is a reliable method. The blue-colored positive signal changes to yellow after addition of the acidic buffer. Positive signals usually have an absorbance reading of >0.500, and negative signals are below 0.050 at 450 nm.

To test the binding specificity of the allele-specific oligonucleotides to the PCR products, different amounts of PCR products from DNAs with different allelic types were applied to the hybridization system. Fig. 1B shows that binding of the oligonucleotides to the corresponding PCR products is specific. As the intensity of the signals increased with the increasing amounts of PCR products, the intensities of the unspecific binding were unchanged.

Analysis of the *p53* polymorphism at codon 72 showed that the proportion of individuals homozygous for arginine, homozygous for proline, and heterozygous for arginine and proline were 54.3%, 7.6%, and 38.1% among the 105 cervical carcinoma patients and 62.4%, 8.3%, and 29.3% among the 133 healthy women (Table 1). χ^2 analysis revealed no significant differences in these proportions between the two groups.

Sequencing of the PCR products from 20 randomly selected samples showed 100% concordance with the results obtained from PCR and allele-specific oligonucleotide hybridization on microtiter plates (data not shown).

In previous studies on the *p53* polymorphism at codon 72, tumor samples were used as the source for DNA *(14–16)*. Although loss of heterozygosity at the *p53* locus is not common in cervical carcinomas, in one study, an allelic imbalance was observed in 22% of the samples *(17)*. Another study demonstrated a loss of heterozygosity rate of 15% on chromosome 17p in cervical carcinomas; the authors suggested that this might be caused by alterations of the *p53* gene *(18)*. The use of DNA from tumor samples for polymorphism analysis may, therefore, lead to inaccurate results. In this study, we used DNA from peripheral blood lymphocytes because they are not affected by such genetic alterations frequently observed in solid tumors.

Comparing the frequencies of allelic variants found in Austrian women with those reported in other Caucasian women (Table 1) *(7, 16)*, both the control group and the carcinoma patients showed no significant differences from the other study groups, indicating that the frequen-

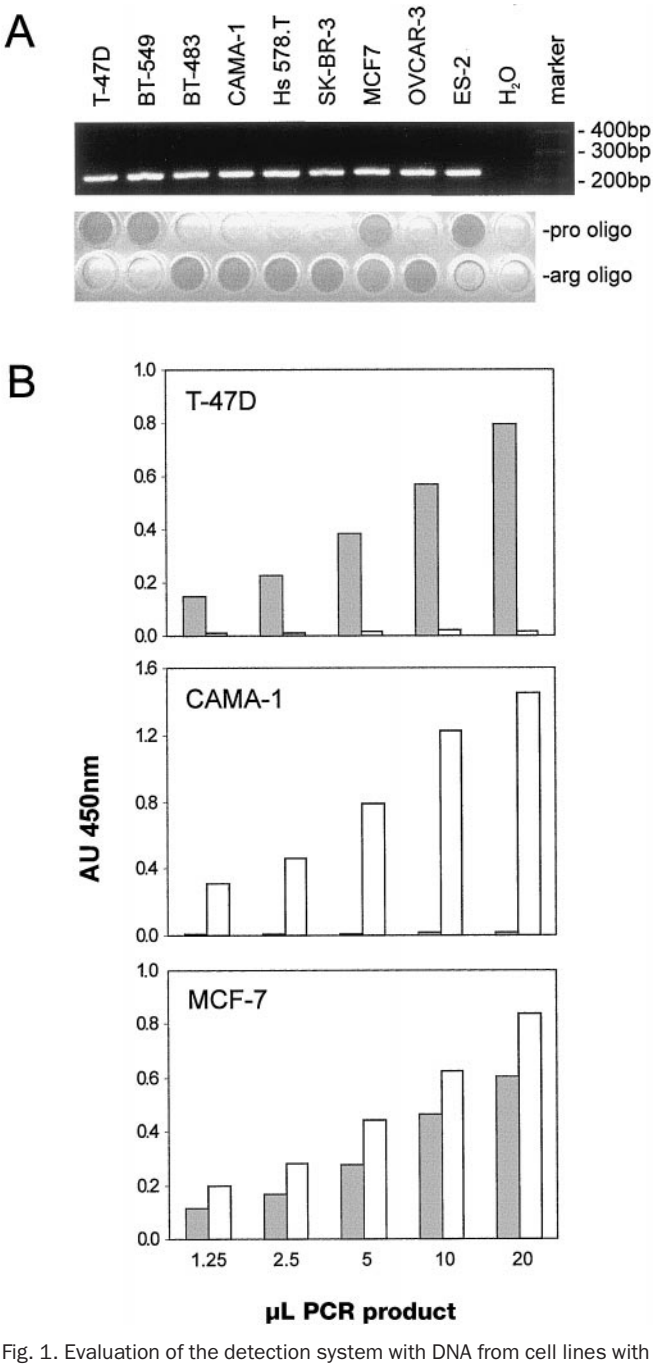

Fig. 1. Evaluation of the detection system with DNA from cell lines with known allelic information (*A*) and specific hybridization of various amounts of PCR products to oligonucleotides specific for the arginine and proline forms (*B*).

(*A*), PCR products on an agarose gel are shown at the *top*; hybridization results for the proline-specific oligonucleotide (*pro oligo*) and arginine-specific oligonucleotide (*arg oligo*) on a microtiter plate are shown at the *bottom*. (*B*), *gray* and *white columns* represent hybridization to proline- and arginine-specific oligonucleotides, respectively. *AU*, absorbance units.

Table 1. Distribution of *p53* allelic variants at codon 72.

	Arg (%)	Pro (%)	Arg/Pro (%)
Cervical carcinomas, n = 105	57 (54.3)	8 (7.6)	40 (38.1)
Control group, n = 133	83 (62.4)	11 (8.3)	39 (29.3)
Sweden,[a] n = 206	110 (53.4)	23 (11.1)	73 (35.4)
United Kingdom,[b] n = 246	155 (63.0)	16 (6.5)	75 (30.5)

[a] From Själander et al. *(7)*.
[b] From Rosenthal et al. *(16)*.

cies of *p53* variants at codon 72 are not different in Caucasian women in Sweden, the United Kingdom, and Austria.

Our results show that there is no difference in the allelic frequencies of the *p53* gene at codon 72 between cervical carcinoma patients and the control group. Because we did not determine HPV status in our study group, we cannot directly compare our results with the data of Storey et al. *(14)*. Storey et al. reported that individuals homozygous for the arginine form at codon 72 are approximately sevenfold more susceptible to HPV-associated cervical cancer than heterozygotes. However, our data are in accordance with the results of two other studies *(15, 16)*, one of which included only cases that were positive for HPV types 16 and 18. Both studies reported a lack of correlation between polymorphism at codon 72 of *p53* and risk of cervical cancer. It cannot be ruled out that such a correlation exists in ethnic groups different from the ones investigated in these studies and ours because a significant difference for the prevalence of arginine homozygotes among various ethnic groups has been reported *(6)*. Therefore, more epidemiological studies that include patients with different ethnic backgrounds should be undertaken. Detection of this *p53* polymorphism with PCR and allele-specific hybridization on microtiter plates is amenable to automation and thus can be very useful for this purpose.

This study was supported by the Anniversary Fund of the Austrian National Bank for the Promotion of Scientific Research and Teaching (Project ÖNB 6054). We thank Andrea Wolf and Sabrina Zeillinger for isolating the DNA used in this study.

References

1. Baker SJ, Markowitz S, Fearon ER, Willson JK, Vogelstein B. Suppression of human colorectal carcinoma cell growth by wild-type *p53*. Science 1990; 249:912–5.
2. Finlay CA, Hinds PW, Levine AJ. The *p53* proto-oncogene can act as a suppressor of transformation. Cell 1989;57:1083–93.
3. Vogelstein B. Cancer. A deadly inheritance. Nature 1990;348:681–2.
4. Milner J, Medcalf EA. Cotranslation of activated mutant *p53* with wild type drives the wild-type p53 protein into the mutant conformation. Cell 1991; 65:765–74.
5. Matlashewski GJ, Tuck S, Pim D, Lamb P, Schneider J, Crawford LV. Primary structure polymorphism at amino acid residue 72 of human p53. Mol Cell Biol 1987;7:961–3.
6. Beckman G, Birgander R, Själander A, Saha N, Holmberg PA, Kivelä A, et al. Is *p53* polymorphism maintained by nature selection? Hum Hered 1994;44: 266–70.
7. Själander A, Birgander R, Saha N, Beckman L, Beckman G. p53 polymorphisms and haplotypes show distinct differences between major ethnic groups. Hum Hered 1996;46:41–8.
8. Birgander R, Själander A, Zhou Z, Fan C, Beckman L, Beckman G. p53 polymorphisms and haplotypes in nasopharyngeal cancer. Hum Hered 1996;46:49–54.
9. Buller RE, Sood A, Fullenkamp C, Sorosky J, Powills K, Anderson B. The influence of the *p53* codon 72 polymorphism on ovarian carcinogenesis and prognosis. Cancer Gene Ther 1997;4:239–45.
10. Kawajiri K, Nakachi K, Imai K, Watanabe J, Hayashi S. Germ line polymorphisms of *p53* and *CYP1A1* genes involved in human lung cancer. Carcinogenesis 1993;14:1085–9.
11. Sarnow P, Ho YS, Williams J, Levine AJ. Adenovirus E1b–58kd tumor antigen and SV40 large tumor antigen are physically associated with the same 54 cellular protein in transformed cells. Cell 1982;28:387–94.
12. Werness BA, Levine AJ, Howley PM. Association of human papillomavirus types 16 and 18 E6 proteins with p53. Science 1990;248:76–9.
13. Scheffner M, Werness BA, Huibregtse JM, Levine AJ, Howley PM. The E6 oncoprotein encoded by human papillomavirus types 16 and 18 promotes the degradation of p53. Cell 1990;63:1129–36.
14. Storey A, Thomas M, Kalita A, Harwood C, Gardiol D, Mantovani F, et al. Role of a p53 polymorphism in the development of human papillomavirus-associated cancer. Nature 1998;393:229–34.
15. Minaguchi T, Kanamori Y, Matsushima M, Yoshikawa H, Taketani Y, Nakamura Y. No evidence of correlation between polymorphism at codon 72 of *p53* and risk of cervical cancer in Japanese patients with human papillomavirus 16/18 infection. Cancer Res 1998;58:4585–6.
16. Rosenthal AN, Ryan A, Al-Jehani RM, Storey A, Harwood CA, Jacobs IJ. *p53* codon 72 polymorphism and risk of cervical cancer in UK. Lancet 1998; 352:871–2.
17. Helland A, Holm R, Kristensen G, Kaern J, Karlsen F, Trope C, et al. Genetic alterations of the *TP53* gene, p53 protein expression and HPV infection in primary cervical carcinomas. J Pathol 1993;171:105–14.
18. Mullokandov MR, Kholodilov NG, Atkin NB, Burk RD, Johnson AB, Klinger HP. Genomic alterations in cervical carcinoma: losses of chromosome heterozygosity and human papilloma virus tumor status. Cancer Res 1996;56:197–205.

Recoveries of Phenylalanine from Two Sets of Dried-Blood-Spot Reference Materials: Prediction from Hematocrit, Spot Volume, and Paper Matrix, *Barbara W. Adam,[1*] J. Richard Alexander,[1] S. Jay Smith,[1] Donald H. Chace,[2] J. Gerard Loeber,[3] L. H. Elvers,[3] and W. Harry Hannon[1]* ([1] Centers for Disease Control and Prevention, Newborn Screening Quality Assurance Program, MS-19, 4770 Buford Hwy., Atlanta, GA 30341-3724; [2] NeoGen Screening, Inc., 110 Roessler Rd., Pittsburgh, PA 15220; [3] Diagnostic Laboratory for Infectious Diseases and Perinatal Screening, National Institute of Public Health and the Environment, P.O. Box 1, 3720 BA Bilthoven, The Netherlands; * author for correspondence: fax 770-488-4831, e-mail bwa1@cdc.gov)

Dried blood spots (DBSs) are used to screen newborns for phenylketonuria and other aminoacidopathies. The calibrators for this testing are usually DBSs with values for Phe. Two DBS reference materials have been prepared, the European Working Standard for Phe (EWS-Phe-01) *(1)* and the amino acid reference material (AARM) from the CDC *(2)*. The two reference materials are not interchangeable because they differ in blood hematocrit, blood-spot size, and filter paper, each of which *(3–6)* affects analyte recovery. We measured quantitatively the effects of these differences on analyte recovery from DBSs and used results from our measurements to predict expected

Phe recoveries from tandem analyses of the two sets of materials.

In EWS-Phe-01 *(1, 7)*, human blood with a 50.5% hematocrit and intact red cells was divided into five portions for enrichment with 0, 20, 40, 80, and 120 mg Phe/L blood (0, 120, 240, 480, and 720 μmol/L blood). The liquid added during enrichment *(7)* was sufficient to reduce the hematocrit to 50.1%. The Phe-enriched blood portions were dispensed in 35-μL aliquots *(7)* onto Schleicher & Schuell (S&S) Grade 2992 (lot no. 121576) filter paper *(1)*.

The AARM was prepared *(2)* by dividing human blood with a 57% hematocrit and intact red cells into six portions for enrichment with pure amino acids to cover the usual analytic ranges of Phe, Tyr, Leu, Met, and Val. The Phe enrichments were 0, 40, 80, 120, 160, and 200 mg Phe/L blood (0, 240, 480, 720, 960, and 1200 μmol/L blood). The liquid added during enrichment was sufficient to reduce the hematocrit to 53%. The whole-blood pools were dispensed in 100-μL portions onto S&S Grade 903 (lot no. W941) filter paper with dashed-line 13-mm printed circles *(2)*.

To examine the effect of blood hematocrit on Phe recovery, we prepared whole-blood portions with 40%, 45%, 50%, 55%, 60%, 65%, and 70% hematocrits from a single batch of packed erythrocytes and a single batch of clarified serum. We enriched the hematocrit-adjusted blood portions with ^{125}I-labeled thyroxine, dispensed 25 100-μL aliquots of each portion onto S&S Grade 903 (lot no. W961) filter paper, and punched ~3 mm (1/8-inch) disks from the north, east, south, west, and center of each dried spot to determine the mean blood absorption volume per disk *(8)* at each hematocrit. We performed a simple linear regression analysis of blood volumes per disk vs hematocrit and used the resulting regression line slope to predict the blood volume of a ~3-mm disk from blood with hematocrits of 53% (the calculated hematocrit of the AARM) and 50.1% (the calculated hematocrit of the EWS-Phe-01).

The EWS-Phe-01 materials were dispensed in 35-μL spots (spot size range, 33–40 μL); the AARMs were dispensed in 100-μL (± 0.24%) spots. To compare Phe recoveries from spot volumes representative of the two sets of materials, we used a single batch of whole blood, adjusted to 55% hematocrit and enriched with 80 mg Phe/L blood, to dispense 35- and 100-μL blood volumes onto S&S Grade 903 (lot no. W941) filter paper. We punched an ~6 mm (1/4-inch) disk from the center of 20 dried spots of each blood volume and measured the Phe concentrations of all of the punched disks in a single HPLC run that was performed according to previously described protocols *(2, 9, 10)*.

To compare the blood absorption characteristics of the S&S filter papers that were used to prepare the EWS-Phe-01 and AARM, we dispensed 100-μL spots of ^{125}I-thyroxine-enriched blood with a 55% hematocrit onto clean, unprinted areas of 10 cards taken from each set of materials. We punched ~3-mm disks from the north, east, south, west, and center of one spot per card for gamma counting in a single analytic run and used a standardized method *(8)* to equate γ counts to the serum volume contained in each DBS disk. We used statistical analyses of the counting data to determine the mean serum-absorption volume per disk for each paper.

We used analyte recoveries computed from our examinations of hematocrit effects, blood-volume-per-spot effects, and filter-paper serum-absorption volumes to predict expected differences between Phe recoveries from the EWS-Phe-01 and the AARM. To evaluate the reliability of the Phe concentration values that were predicted from measurements of matrix variables, we analyzed the EWS-Phe-01 and the AARM in duplicate in each of five HPLC runs and compared the mean values of the measured Phe concentrations with the predicted Phe concentrations. We also compared regression slopes, derived from measured vs enriched Phe concentrations of each set of DBS materials, to show the ratio of their measured Phe recoveries.

Studies of hematocrit effects showed that the blood volume per ~3-mm disk was positively correlated with the hematocrit. The slope of the regression line, derived from measured blood volume per disk vs hematocrit, predicted that the EWS-Phe-01 materials, with a calculated hematocrit of 50.1%, should have a blood volume of 3.1 μL per ~3-mm disk, whereas the AARM, with a 53% calculated hematocrit, should have a blood volume of 3.2 μL per disk.

In studies of the effect of blood volume per spot on analyte recovery, the total Phe concentration of the blood used was equal to the endogenous Phe, which was not measured, plus the Phe enrichment. The mean of recovered Phe concentrations from the 35-μL spots (85.1 ± 4.7 mg/L blood) was lower than that from the 100-μL spots (95.5 ± 9.1 mg/L blood; $P < 0.01$, Student *t*-test).

The mean serum-absorption volume per ~3-mm disk punched from the S&S Grade 2992 paper used to prepare the EWS-Phe-01 was 1.250 ± 0.104 μL, whereas that from the S&S Grade 903 paper used to prepare the AARM was 1.502 ± 0.188 μL ($P < 0.01$).

The controlled comparisons of hematocrits, blood volumes per spot, and filter-paper serum-absorption volumes showed, in all cases, that analyte recovery per DBS disk was lower for the conditions used in the preparation of EWS-Phe-01 than from those used in the preparation of AARM. By summing these observed differences, we projected (Table 1) that analyte recovery from EWS-Phe-01 and AARM could be expected to differ by 30.8% when the two sets of materials were analyzed in tandem. By comparing the regression slopes derived from HPLC-measured vs enriched Phe concentrations of each set of DBS materials, we found that observed Phe recoveries from EWS-Phe-01 (regression slope, 0.698) were 31.6% lower than those from AARM (regression slope, 1.020) when the two sets of reference materials were analyzed in tandem against the same set of calibrators. Our HPLC calibration and data-reduction protocol was that provided by the manufacturer to newborn-screening laboratories in the United States. This protocol yields ~100% Phe recovery from 100-μL spots of intact-cell blood dispensed onto S&S Grade 903 filter paper; therefore, Phe recoveries from the

Table 1. Differences in analyte recoveries related to the hematocrits, blood volumes per spot, and filter papers used to prepare EWS-Phe-01 and AARM.

Compared element	Analyte recoveries	Ratios of analyte recoveries	Difference in analyte recoveries, %
Hematocrit effect on blood volume per ~3-mm disk punched from a 100-μL dried-blood spot on S&S Grade 903 paper	3.1 μL of blood per ~3-mm disk at hematocrit (50.1%) used to prepare EWS-Phe-01 3.2 μL of blood per ~3-mm disk at hematocrit (53%) used to prepare AARM	$\frac{3.1\ \mu L}{3.2\ \mu L} = 0.969$	3.1
Blood-spot volume effect on Phe recovery from an ~6-mm disk punched from the center of a spot of blood enriched with 80 mg Phe/L blood	85.1 mg Phe/L blood recovered from blood spots of the 35-μL size used to prepare EWS-Phe-01 95.5 mg Phe/L blood recovered from blood spots of the 100-μL size used to prepare AARM	$\frac{85.1\ mg/L}{95.5\ mg/L} = 0.891$	10.9
Filter paper effect on serum volume per ~3-mm disk punched from a 100-μL spot of 55% hematocrit blood	1.250 μL of serum per ~3-mm disk punched from blood spots on the S&S 2992 paper used to prepare EWS-Phe-01 1.502 μL of serum per ~3-mm disk punched from blood spots on the S&S 903 paper used to prepare AARM	$\frac{1.250\ \mu L}{1.502\ \mu L} = 0.832$	16.8
Sum of observed differences			30.8

AARM were expected to equal the AARM target values *(2)*. Conversely, in an analytic system with calibration and data-reduction protocols appropriate for European newborn-screening samples, Phe recoveries from the EWS-Phe-01 would be expected to equal the EWS-Phe-01 target values *(1)*.

The effects of the differences in the blood hematocrit, blood volume per spot, and filter-paper sources used to prepare the EWS-Phe-01 and AARM yielded analytic recovery differences of 3.1%, 10.9%, and 16.8%, respectively. These relationships between blood-spot preparation variables and analytic recovery illustrate the importance of (*a*) preparing reference materials for newborn-screening tests from blood with a hematocrit typical of newborns and in spot sizes similar to those of the newborn-screening specimens and on the same filter paper grade and lot number used for collecting the newborn-screening samples, and (*b*) considering the blood-spot preparation variables when comparing different sets of blood-spot reference materials.

The EWS-Phe-01 and AARM were prepared from blood with hematocrits typical of newborns and with filter papers and blood-spot sizes that reflect newborn-screening practices in the regions in which they are used. Because of the observed matrix-related differences in analyte recoveries, we predicted that Phe recoveries from tandem analyses of the EWS-Phe-01 and AARM would be 30.8% higher from the AARM. In fact, measured Phe concentrations from the AARM were 31.6% higher than those from the EWS-Phe-01 when the materials were analyzed in tandem. We conclude that controlled measurements of blood-spot preparation variables can be used to reliably predict analyte recoveries from DBS materials, and we have shown that the Phe contents of the EWS-Phe-01 and AARM are concordant when the effects of their preparation variables are normalized; thus we verified the suitability of the materials as calibrators for their respective regions.

The effects of blood-spot preparation variables are not limited to phenylketonuria tests or to newborn screening. Investigators who use DBSs must be aware of the variables that affect blood-spot test results. Knowledge of the relationship between reference materials and DBS test samples and awareness of the relationships among different sets of reference materials are essential for evaluating test results, comparing data among laboratories, and evaluating laboratory performance in different areas of the world.

References

1. Dhondt JL, Loeber JG, Elvers LH, Paux E. Preparation of the first European working standard for phenylalanine determination in dried blood spots. J Med Screen 1998;5:63–6.
2. Chace DH, Adam BW, Smith JS, Alexander JR, Hillman SL, Hannon WH. Validation of accuracy-based amino acid reference materials in dried-blood spots by tandem mass spectrometry for newborn screening assays. Clin Chem 1999;45:1269–77.
3. Jensen RJ, Adam BW, Turner W, Hannon WH. An evaluation of different filter paper lots used for blood spot specimen collection during the last five years. In: Chan MS, ed. Proceedings of the National Newborn Screening Symposium, February 7–9, 1984, Orlando, Florida (USA). Jacksonville, FL: Department of Health and Rehabilitative Services, 1984:15–29.
4. Hannon WH, Mei JV, Adam BW. Contending with specimen collection paper from different commercial sources while maintaining quality performance. In: Glass M, ed. Proceedings of the 10th National Neonatal Screening Symposium, Seattle, Washington (USA). Seattle, Washington: Association of State and Territorial Laboratory Directors, 1994:165–6.
5. Elvers LH, Loeber JG. The need for standardized bloodspot TSH-calibrators in congenital hypothyroidism screening. Early Hum Dev 1996;45:179–90.
6. Dhondt JL, Paux E, Farriaux JP. Need for a standardized procedure in the preparation of phenylalanine calibrators. Early Hum Dev 1996;45:277–85.
7. Elvers LH, Loeber JG, Dhondt JL. Preparation of the first European working standard for phenylalanine in dried blood spots: EWS-Phe-01. RIVM Report No. 199003047. Bilthoven, The Netherlands: RIVM, 1996.
8. Hannon WH, Boyle J, Davin B, Marsden A, McCabe ERB, Schwartz, M, et al. Blood collection on filter paper for neonatal screening programs; 3rd ed., approved standard. NCCLS Document LA4-A3. Wayne, PA: NCCLS, 1997.
9. Cohen SA, Michaud DP. Synthesis of a fluorescent derivatizing reagent, 6-aminoquinolyl-*N*-hydroxysuccinimidyl carbamate, and its application for the analysis of hydrolysate amino acids via high-performance liquid chromatography. Anal Biochem 1993;211:279–87.
10. Cohen SA, van Wandelin C. A new HPLC method for the quantitative determinations of clinically relevant amino acids from bloodspots. In: Therrell BL Jr, Aldis BG, eds. Proceedings of the 11th National Neonatal Screening Symposium, Corpus Christi, Texas (USA). Austin, TX: Association of State and Territorial Public Health Laboratory Directors, 1995:253–5.

Rapid Method for Detection of Extra (TA) in the Promoter of the Bilirubin-UDP-Glucuronosyl Transferase 1 Gene Associated with Gilbert Syndrome, *Doroti Pirulli,[1] Mara Giordano,[2] Daniela Puzzer,[1] Sergio Crovella,[1] Igino Rigato,[3] Claudio Tiribelli,[3] Patricia Momigliano-Richiardi,[2] and Antonio Amoroso[1*]* ([1] Servizio di Genetica Medica, Instituto di Ricovero e Cura a Carattere Scientifico Burlo Garofolo and Università di Trieste, 34137 Trieste, Italy; [2] Dipartimento di Scienze Mediche, Università degli Studi del Piemonte Orientale "Amedeo Avogadro", Novara 28100, Italy; [3] Dipartimento di Biochimica, Biofisica e Chimica delle Macromolecole, Università di Trieste, 34137 Trieste, Italy; * address correspondence to this author at: Servizio di Genetica, IRCCS Burlo Garofolo, Via dell'Istria, 65/1, 34137 Trieste, Italy; fax 39-040-3785210, e-mail amoroso@burlo.trieste.it)

Gilbert syndrome (GS) is an inherited form of chronic mild unconjugated hyperbilirubinemia *(1–3)*, although many patients do not have a clear family history *(4)*. Hepatic glucuronidation of bilirubin is catalyzed by isoenzyme 1A1 of UDP-glucuronosyl transferase (UGT1A1). The majority of GS subjects were found to be homozygous for an extra TA in the TATA-box in the promoter region of *UGT1A1 (5–7)*. Transcription of the (TA)7 allele is reduced by at least 70% compared with the wild-type (TA)6 allele. Because bilirubin UGT1A1 is the only enzyme with substantial bilirubin glucuronidating activity in humans *(8)*, the presence of this extra TA in both alleles can explain the impaired conjugation of bilirubin found in Caucasoid GS patients *(6)*.

A previous study of a large population found that the prevalence of the "abnormal" bilirubin *UGT1A1* allele was 35–40% *(9)*, leading to an expected frequency of homozygotes of ~16%; however, only 5% had increased serum concentrations of unconjugated bilirubin. Thus, a reduced expression of bilirubin UGT1A1, attributable to the (TA)7 abnormality in the promoter region, appears to be necessary, but not sufficient, for GS to be manifested clinically.

To date, the TA polymorphism has been detected by PCR amplification of the TATA-box element and high resolution polyacrylamide gel electrophoresis *(9)* or by direct sequencing *(6)*. Recently, a new technique for sensitive, relatively inexpensive and automated high-throughput screening of mutations, denaturing HPLC (DHPLC), was introduced *(10–13)*. In this report, we evaluate the feasibility of applying DHPLC for the detection of TATA-box variants in the promoter region of the *UGT1A1* gene in subjects with GS.

The *UGT1A1* promoter was analyzed by both DHPLC and direct sequencing in 20 unrelated GS patients (16 males and 4 females; age range, 16–40 years) and 20 healthy controls with bilirubin concentrations within the reference interval (16 males and 4 females; age range, 13–35 years). The diagnosis of GS was based on the standard criteria of mild chronic, unconjugated hyperbilirubinemia in the presence of normal liver function and the absence of overt signs of hyperhemolysis (erythrocyte and reticulocyte counts, erythrocyte osmotic fragility, and immunoelectrophoretic patterns of erythrocyte hemoglobin were all normal) *(14)*. None of the subjects had a history of hepatic or hematological disorders, excessive alcohol intake, or chronic use of medications or narcotics, and none received any drug during the 2 weeks before investigation.

In each subject, after an overnight fast, plasma concentrations of total and direct-reacting bilirubin were determined by a diazo method at least three times within 6 months before the study; indirect bilirubin was calculated as total minus direct bilirubin. Control subjects were pair-matched for age and sex. After informed consent, each patient and control was analyzed by both sequencing and DHPLC by investigators "blinded" to the plasma bilirubin concentrations.

DNA was isolated from EDTA-collected peripheral whole blood, using standard laboratory techniques *(15)*.

The PCR reactions were performed in a 50-μL final volume containing 8 pmol of each primer, as described *(6)*, and 1 U of AmpliTaq GOLD DNA polymerase (PE Applied Biosystems) in a thermal cycler 2400 (PE Applied Biosystems). After 35 cycles, PCR products were detected in a 2% agarose gel.

Heteroduplex molecules originate when a variation at the heterozygous state is present in a DNA fragment after denaturing and reannealing of the PCR product. DHPLC is based on the differential retention of homoduplex and heteroduplex molecules under the condition of partial heat denaturation. At low temperatures (50 °C), the two molecular types usually are coeluted. At increasing temperatures, the DNA starts to melt selectively in the region of mismatch of the heteroduplexes. Under these conditions, heteroduplex molecules are eluted ahead of homoduplexes, producing an additional peak.

To allow heteroduplex formation, PCR products were denatured for 3 min at 95 °C, followed by a gradual reannealing as temperature was decreased from 95 °C to 65 °C over 30 min in the thermal cycler. The reannealed duplexes were detected by scanning on an automated HPLC (Transgenomics). The stationary phase consisted of 2-μm nonporous alkylated poly(styrene-divinylbenzene) particles packed into a 50- × 4.6-mm (i.d.) column.

A 3- to 5-μL aliquot of each PCR product was injected onto the column and eluted at a flow rate of 0.9 mL/min with a mobile phase consisting of a mixture of buffers A and B; buffer A was 0.1 mol/L triethylammonium acetate (pH 7) and buffer B was 250 mL/L acetonitrile in 0.1 mol/L triethylammonium acetate (pH 7). The optimal temperature for HPLC was determined experimentally as 56 °C, and the PCR product separation was achieved through the following gradient: buffer B was increased from 57% to 62% over 30 s and then from 62% to 70% over 4 min. The eluted DNA fragments were detected at 260 nm.

DNA sequencing was performed on an automated ABI Prism 310 Genetic Analyzer (PE Applied Biosystems) with a BigDye Terminator Cycle Sequencing Ready Reaction Kit (PE Applied Biosystems) using forward and reverse primers *(16)*.

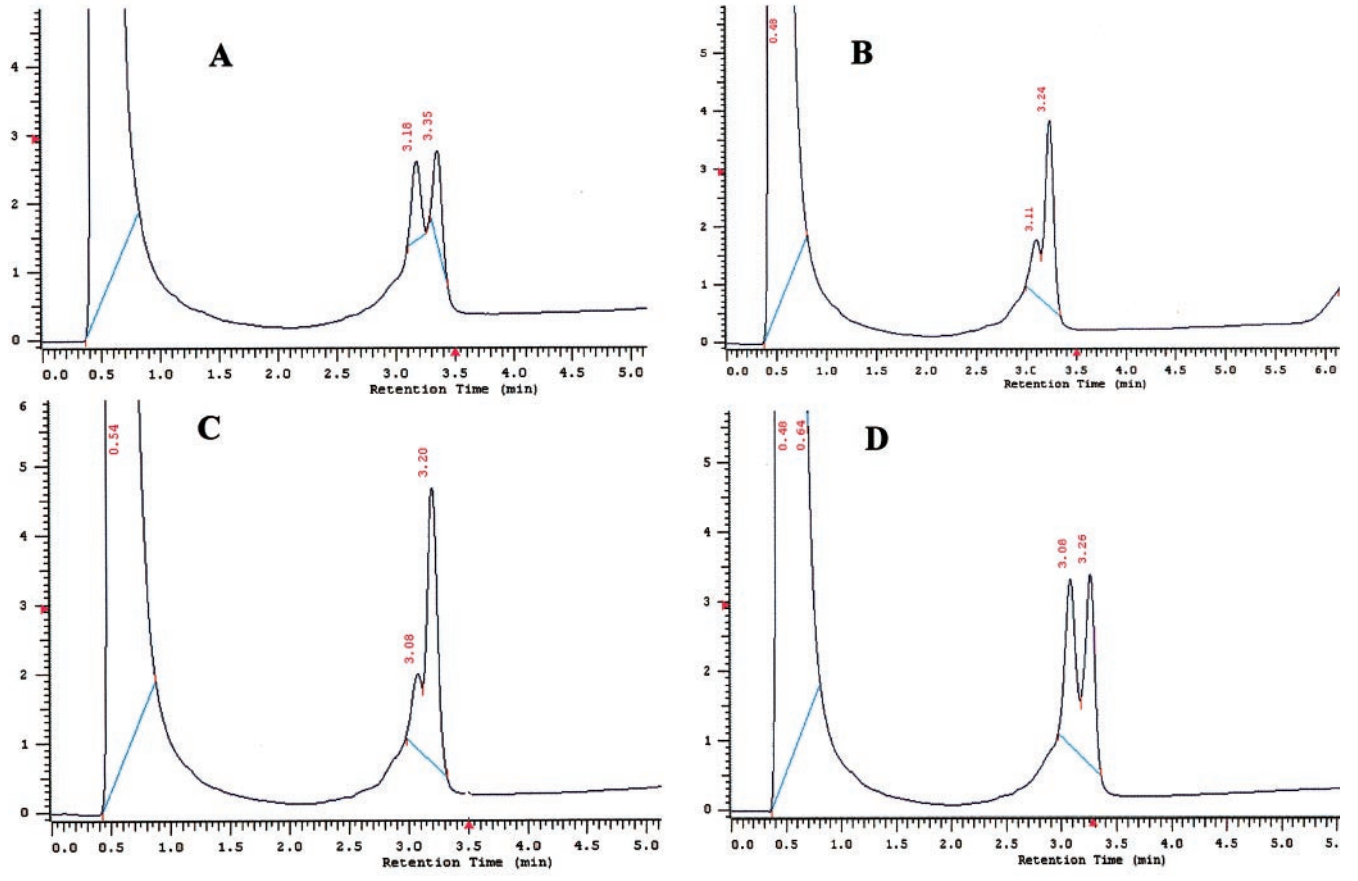

Fig. 1. Chromatograms obtained after amplification of the upstream region of the *UGT1A1* gene in subjects showing different genotypes according to the number of (TA) repeats.

(*A*), DHPLC pattern of a heterozygous (TA)6/(TA)7 individual, showing two well-resolved peaks. (*B* and *C*), the homozygous conditions (TA)6/(TA)6 (*B*) or (TA)7/(TA)7 (*C*) cannot be distinguished from one another by observing the peaks. To identify the (TA)7 homozygotes, each sample showing a single peak was mixed with a (TA)6/(TA)6 control DNA, denatured for 3 min at 95 °C, and gradually reannealed from 95 °C to 65 °C to generate heteroduplex molecules. The homozygous condition for (TA)7 was revealed by a double peak, as shown in *panel D*, that was identical to that observed in heterozygous individuals.

The mean (± SD) total serum bilirubin concentrations of GS subjects was 15.5 ± 4.0 mg/L, significantly ($P < 0.001$) higher than in controls (6.6 ± 2.4 mg/L). In both controls and GS subjects, >80% of bilirubin was indirect reacting.

PCR products of a promoter region (from nucleotide −227 to nucleotide 132) containing the TATA-box element, were analyzed by DHPLC. The presence of two well-resolved peaks in Fig. 1A reveals the heterozygous condition (TA)6/(TA)7, as confirmed by direct sequencing. The presence of one peak is characteristic of the homozygous condition (Fig. 1, B and C). To distinguish (TA)6 from (TA)7 homozygotes, each sample showing a single peak was mixed with (TA)6/(TA)6 control DNA under conditions allowing heteroduplex formation. The homozygous condition for (TA)7 was revealed by a double peak (Fig. 1D), whereas no change in the chromatogram showing a single peak was detected for (TA)6 homozygotes. DHPLC results showed a 100% match with those obtained by direct sequencing.

The genotype frequencies in both Gilbert patients and controls are reported in Table 1. This distribution in healthy controls was significantly different from that expected by Hardy-Weinberg law ($\chi^2 = 4.3$; $P < 0.05$), mainly because of a higher than expected number of homozygotes. The (TA)7 allele was significantly more frequent in GS subjects than in controls (0.9 vs 0.25; $\chi^2 = 34.5$; $P < 0.00001$).

Several useful techniques for detecting mutations have evolved in recent years. The most widely used simple single-step analytical method, single-strand conformational polymorphism, has a low sensitivity, whereas the

Table 1. Genotype frequencies of TA repeats in the promoter region of *UGT1A1*, as revealed by DHPLC or direct sequencing, in Gilert patients and healthy controls.

	Frequency, %	
Genotypes	Gilbert patients (n = 20)	Healthy controls (n = 20)
(TA)7	80	15[a]
(TA)6/(TA)7	20	20
(TA)6	0	65[a]

[a] $P < 0.00001$.

more sensitive methods (i.e., direct sequencing and denaturing gradient gel electrophoresis) are often expensive and time-consuming *(11)*.

As illustrated in our study, DHPLC technology for detection of mutants is a powerful and sensitive tool useful for the rapid, efficient screening of large numbers of samples. We found 100% concordance with direct sequencing, and the reagent costs of a DHPLC analysis (~$3 US per sample, PCR included) are lower than those of direct sequencing ($15 US). The labor requirements and operator time are also reduced, further increasing the cost-effectiveness. After temperature optimization, automated DHPLC analysis requires only a few seconds to load the autosampler and ~5 min to run each sample. The interpretation of the final chromatograms is also rapid. If a single peak is detected, however, a second run must be performed, with the PCR product mixed with a known homozygous control, to differentiate the two homozygous genotypes.

In the limited numbers of subjects in our study, we confirmed that the (TA)7 variation was significantly more frequent in GS subjects than in controls. The absence of Hardy-Weinberg equilibrium in controls may result from the small sample of individuals studied or from selection bias.

In conclusion, DHPLC can be chosen as a large-scale screening method for detection of the (TA)7 mutation in the promoter region of the *UGT1A1* gene. It may be helpful in determining whether impaired glucuronidation contributes to clinical hyperbilirubinemia in subjects with abnormalities in bilirubin metabolism, as in subjects with heterozygous β-thalassemia *(17)*, glucose-6-phosphate dehydrogenase deficiency *(18)*, neonatal icterus associated with glucose-6-phosphate dehydrogenase deficiency *(19)*, or hereditary spherocytosis *(20)*.

This work was supported in part by a grant from the Italian Ministry of Research Ministero dell'Università per la Ricerca Scientifica e Tecnologia (to C.T.) and grants from the Italian Ministry of Health (Grants RC 19/99 and RF 98.67 to A.A.). D. Pirulli is the recipient of a long-term fellowship from the University of Trieste. D. Puzzer is a recipient of a fellowship from Children's Hospital Burlo Garofolo of Trieste. The financial support of Fondo Studi Fegato-ONLUS, Trieste, is also acknowledged. We thank Drs. J.D. Ostrow and J. Mihelcic for constructive discussions during the preparation of this manuscript.

References

1. Foulk WT, Butt HR, Owen CA Jr, Whitcomb FF, Mason HL. Constitutional hepatic dysfunction (Gilbert's disease): its natural history and related syndromes. Medicine 1959;38:25–46.
2. Powell LW, Hemingway E, Billing BH, Sherlock S. Idiopathic unconjugated hyperbilirubinemia (Gilbert's syndrome). A study of 42 families. N Engl J Med 1967;277:1108–12.
3. Berk PD, Martin JF, Blaschke TF, Scharschmidt BF, Plotz PH. Unconjugated hyperbilirubinemia: physiologic evaluation and experimental approaches to therapy. Ann Intern Med 1975;82:552–70.
4. Thompson RPH. Genetic transmission of Gilbert's syndrome. In: Okolicsanyi L, ed. Familial hyperbilirubinemia. New York: John Wiley, 1981:91–7.
5. Koiwai O, Nishizawa M, Hasada K, Aono S, Adachi Y, Mamiya N, Sato H. Gilbert's syndrome is caused by a heterozygous missense mutation in the gene for bilirubin UDP-glucuronosyltransferase. Hum Mol Genet 1995;4: 1183–6.
6. Bosma PJ, Roy Chowdhury J, Bakker CTM, Gantla S, de Boer A, Oostra BA, et al. The genetic basis of the reduced expression of bilirubin UDP-glucuronosyltransferase 1 in Gilbert's syndrome. N Engl J Med 1995;333: 1171–5.
7. Beutler E, Gelbart T, Demina A. Racial variability in the UDP-glucuronosyltransferase 1 (*UGT1A1*) promoter: a balanced polymorphism for regulation of bilirubin metabolism? Proc Natl Acad Sci U S A 1998;95:8170–4.
8. Bosma PJ, Seppen J, Goldhoorn B, Bakker C, Oude Elferink RPJ, Roy Chowdhury J, et al. Bilirubin-UDP-glucuronosyltransferase 1 is the only relevant bilirubin glucuronidating isoform in man. J Biol Chem 1994;269: 17960–4.
9. Sampietro M, Lupica L, Perrero L, Romano R, Molteni V, Fiorelli G. TATA-box mutant in the promoter of the uridine diphosphate glucuronosyltransferase gene in Italian patients with Gilbert's syndrome. Ital J Gastroenterol Hepatol 1998;30:194–8.
10. Underhill PA, Jin L, Lin AA, Mehdi SQ, Jenkins T, Vollrath D, et al. Detection of numerous Y chromosome biallelic polymorphisms by denaturing high performance liquid chromatography (DHPLC). Genome Res 1997;7:996–1005.
11. O'Donovan MC, Oefner PJ, Roberts SC, Austin J, Hoogendoorn B, Guy C, et al. Blind analysis of denaturing high-performance liquid chromatography as a tool for mutation detection. Genomics 1998;52:44–9.
12. Liu W, Smith DI, Rechtzigel KJ, Thibodeau SN, James CD. Denaturing high performance liquid chromatography (DHPLC) used in the detection of germline and somatic mutations. Nucleic Acids Res 1998;26:1396–400.
13. Giordano M, Oefner PJ, Underhill PA, Cavalli-Sforza LL, Tosi R. Momigliano Richiardi P. Identification by denaturing high performance liquid chromatography (DHPLC) of numerous polymorphisms in a candidate region for multiple sclerosis susceptibility. Genomics 1999;56:247–53.
14. Gentile S, Orzes N, Persico M, Marmo R, Bronzino P, Tiribelli C. Comparison of nicotinic acid- and caloric restriction-induced hyperbilirubinaemia in the diagnosis of Gilbert's syndrome. J Hepatol 1985;1:537–43.
15. Sambrook J, Fritsch T, Maniatis T. Molecular cloning, 2nd ed. Cold Spring Harbor, NY: Cold Spring Harbor Laboratory, 1989:1659 pp.
16. Rosenthal A, Chamock JDS. New protocols for DNA sequencing with dye terminators. DNA Seq 1992;3:61–4.
17. Galanello R, Perseu L, Melis MA, Cipollina L, Barella S, Giagu N, et al. Hyperbilirubinaemia in heterozygous β-thalassaemia is related to co-inherited Gilbert's syndrome. Br J Haematol 1997;99:433–6.
18. Sampietro M, Lupica L, Perrero L, Comino A, Martinez di Montemuros F, Cappellini MD, Fiorelli G. The expression of uridine diphosphate glucuronosyltransferase gene is a major determinant of bilirubin level in heterozygous β-thalassaemia and in glucose-6-phosphate dehydrogenase deficiency. Br J Haematol 1997;99:437–9.
19. Kaplan M, Renbaum P, Levy-Lahad E, Hammerman C, Lahad A, Beutler E. Gilbert syndrome and glucose-6-phosphate dehydrogenase deficiency: a dose-dependent genetic interaction crucial to neonatal hyperbilirubinemia. Proc Natl Acad Sci U S A 1997;94:12128–32.
20. Iolascon A, Faienza MF, Moretti A, Perrotta S, Miraglia del Giudice E. *UGT1* promoter polymorphism accounts for increased neonatal appearance of hereditary spherocytosis [Letter]. Blood 1998;91:1093.